LETTERS

Control of segment number in vertebrate embryos

Céline Gomez[1], Ertuğrul M. Özbudak[1], Joshua Wunderlich[1], Diana Baumann[1], Julian Lewis[2] & Olivier Pourquié[1,3]

The vertebrate body axis is subdivided into repeated segments, best exemplified by the vertebrae that derive from embryonic somites. The number of somites is precisely defined for any given species but varies widely from one species to another. To determine the mechanism controlling somite number, we have compared somitogenesis in zebrafish, chicken, mouse and corn snake embryos. Here we present evidence that in all of these species a similar 'clock-and-wavefront'[1–3] mechanism operates to control somitogenesis; in all of them, somitogenesis is brought to an end through a process in which the presomitic mesoderm, having first increased in size, gradually shrinks until it is exhausted, terminating somite formation. In snake embryos, however, the segmentation clock rate is much faster relative to developmental rate than in other amniotes, leading to a greatly increased number of smaller-sized somites.

Vertebrate segments are formed during early embryogenesis, when vertebrae precursors, called somites, bud off in a rhythmic fashion from the anterior part of the presomitic mesoderm (PSM). The periodic formation of somites is proposed to be controlled by a molecular oscillator—the segmentation clock—which drives the periodic activation of the Notch, Wnt and fibroblast growth factor (FGF) pathways in the PSM[1,2,4]. The periodic signal of the segmentation clock is converted into a repetitive series of somites by a travelling front of maturation—the wavefront or determination front—formed by a Wnt/FGF signalling gradient that regresses caudally in the PSM in concert with axis elongation[5–8].

The number of somites, and hence of vertebrae, is highly variable among vertebrate species[9]. For instance, frogs have ~10 vertebrae, whereas humans have 33 and snakes can have more than 300. To investigate the mechanisms controlling somite numbers in vertebrates, we compared somitogenesis in the corn snake (*Pantherophis guttatus*; Fig. 1a, b), which makes a large number of somites (~315), with that in three other vertebrate species that make far fewer: zebrafish (*Danio rerio*, 31), chicken (*Gallus gallus*, 55) and mouse (*Mus musculus*, 65).

We examined the expression of the corn snake homologues of genes involved in PSM patterning and somitogenesis (Fig. 2a–l). The genes coding for fibroblast growth factor 8 (FGF8) (Fig. 2b) and its targets sprouty 2 (SPRY2; Fig. 2c) and dual specificity phosphatase 6 (DUSP6)[4,10] (Fig. 2d), as well as WNT3A (Fig. 2e) and its targets AXIN2 (ref. 7; Fig. 2f) and mesogenin 1 (MSGN1) (ref. 11; Fig. 2g), ephrin receptor A4 (EPHA4; Fig. 2h), the retinoic acid biosynthetic enzyme (RALDH2; Fig. 2i), paraxis (TCF15) (Fig. 2j), UNCX4.1 and MYOD (Supplementary Fig. 1) were cloned and their expression analysed by *in situ* hybridization. All of these genes (except *SPRY2*) were expressed in domains comparable to those observed in their fish or amniote counterparts[4–7,12–19], supporting the existence of a Wnt/FGF posterior gradient opposing an anterior retinoic acid gradient in corn snake, as in other species.

We compared the dynamics of this gradient in snake with that in the other species. As a readout for the posterior gradients, we used *MSGN1* expression, which is controlled by the Wnt/FGF gradient

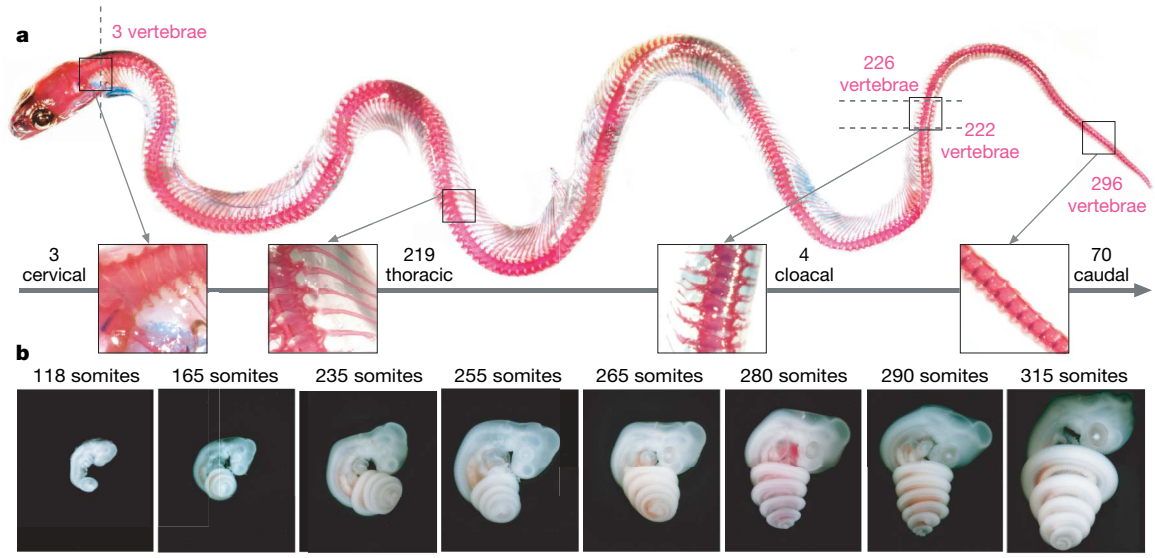

Figure 1 | Vertebral formula and somitogenesis in the corn snake. **a**, Alizarin staining of a corn snake showing 296 vertebrae, including 3 cervical, 219 thoracic, 4 cloacal (distinguishable by their forked lymphapophyses) and 70 caudal. **b**, Time course of corn snake development after egg laying (118-somite embryo on the far left) until the end of somitogenesis (~315 somites).

[1]Stowers Institute for Medical Research, Kansas City, Missouri 64110, USA. [2]Vertebrate Development Laboratory, Cancer Research UK, London Research Institute, London WC2A 3PX, UK. [3]Howard Hughes Medical Institute, Kansas City, Missouri 64110, USA.

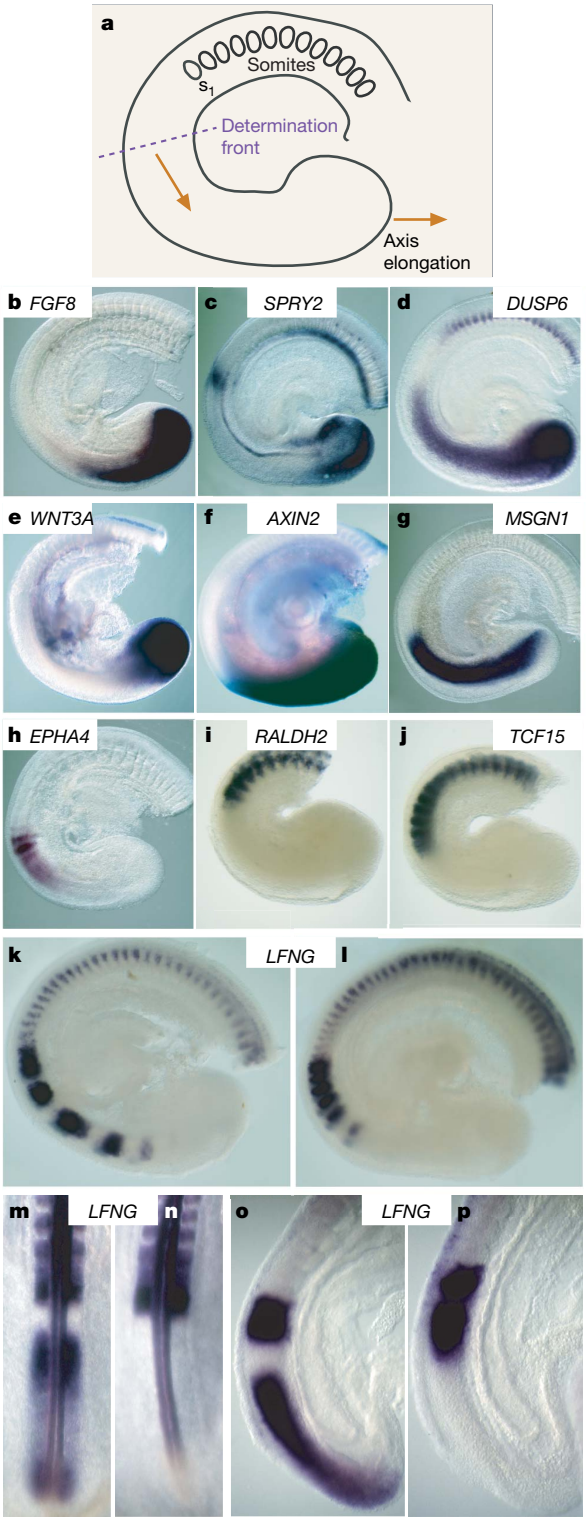

Figure 2 | The corn snake determination front and segmentation clock. **a**, Schematic drawing of a corn snake tail showing the position of the determination front (dashed line) in the PSM relative to the newly formed somite (s_1). **b–l**, Whole-mount *in situ* hybridizations of 230-somite (**b–h**, **k**, **l**) and 260-somite (**i**, **j**) corn snake embryo tails: *FGF8* (**b**), *SPRY2* (**c**), *DUSP6* (**d**), *WNT3A* (**e**), *AXIN2* (**f**), *MSGN1* (**g**), *EPHA4* (**h**), *RALDH2* (**i**) and *TCF15* (**j**). Two different phases of *LFNG* expression in 230-somite corn snake embryos (**k**, **l**), two-day-old chicken embryos (**m**, **n**) and E9.5 mouse embryos (**o**, **p**). Lateral views in **a–l**, **o** and **p**. Dorsal views in **m** and **n**. Anterior to the top.

and for which the sharp anterior boundary marks the position of the mesoderm posterior 2 (*MESP2*) stripe[20] at the determination front[3] (Fig. 2a–g). We measured the regression speed of the *MSGN1* anterior boundary during somitogenesis in all four species (Fig. 3a–x) and found that it moves by one somite length during one period of somite formation, independent of the somitogenesis stage and the species (Fig. 4a and Supplementary Fig. 2). This validates an important prediction of the clock-and-wavefront model—that somite size corresponds to the distance travelled by the wavefront during one oscillation period. We plotted the ratio of *MSGN1* expression domain to PSM size as a function of stage for each species (Fig. 4b). Notably, a similar ratio was observed throughout somitogenesis in all four species, suggesting that similar processes (scaled proportionately) are occurring. Thus, the characteristics of the gradient system involved in PSM patterning seem to be conserved between corn snake and the other species examined.

We examined the cyclic gene expression associated with the amniote segmentation clock. No dynamic expression of *SPRY2*, *DUSP6* (ref. 4) or *AXIN2* (ref. 7) was evident in the snake PSM (Fig. 2c, d, f). However, *Lunatic fringe* (*LFNG*) exhibited an unexpected expression pattern that consisted of up to nine stripes of variable size and spacing in the PSM (Fig. 2k, l)[21,22]. Thirty-nine snake embryos were hybridized with *LFNG* and all showed a different expression pattern (Fig. 2k, l and data not shown). These data support the existence of an oscillator driving cyclic gene expression in snake embryos. The number of stripes of *LFNG* expression in corn snake is, however, several times larger than in other vertebrate species (Fig. 2k–p), suggesting that the segmentation clock might be regulated in a different way.

Assuming that one somite is formed during each clock oscillation cycle, we can deduce the period of the clock oscillations by counting somite numbers in embryos from the same clutch at various incubation times (Supplementary Methods). In the corn snake, the average somite formation rate is one pair every 100 min, compared to rates of one pair every 30, 90 and 120 min in zebrafish, chicken and mouse, respectively. The somite formation rate was found to be one pair every ~60 min in the house snake (*Lamprophis fuliginosus*) embryos, which has very similar developmental characteristics and *LFNG* expression pattern to the corn snake (Supplementary Methods and Supplementary Fig. 3).

To appreciate the significance of these periods, we need to compare them to the general rate of development, which differs between species. Comparison of the time required to reach conserved morphological landmarks (Supplementary Fig. 4) suggests that the development rate is at least three times slower in corn snake than in chicken. We also examined the lizard *Aspidoscelis uniparens*, which has the same slow general development rate as the snake[23] (Supplementary Methods). This species makes only ~90 somites and has a much longer somite formation time (~4 h). Therefore, relative to the development rate, the clock ticks much faster in snake than in chicken or lizard embryos.

Analysing the relationship between somitogenesis rate and growth rate of the PSM tissue confirms this hypothesis. According to the clock-and-wavefront model, each somite consists of the cells emerging from the PSM in one clock cycle. This must equal the quantity of new cells generated in the PSM by growth, at least when the PSM maintains a steady size. Thus, the somite size as a fraction of the PSM size directly reflects the duration of the clock cycle as a fraction of the average PSM cell generation time (that is, average cell-cycle time; Supplementary Box 1). In snake, this fraction is approximately one-quarter of the value observed in other species (Fig. 4c). Thus, the snake segmentation clock runs approximately four times faster relative to the average PSM cell generation time than in the other species.

We estimated the average cell generation time and the total number of PSM cell generations required to produce a complete set of somites. For this, we took into account the way in which the PSM size

changes over the course of somitogenesis (Figs 3a–x and 4d). In zebrafish, the PSM length decreases from the beginning of somitogenesis; in amniote embryos, the PSM first increases and then decreases in size until somitogenesis ends[24] (Fig. 4d). From the detailed measurements of PSM length and the size of the most recently formed somite s_1 as a function of developmental stage (Fig. 4d, e), combined with a knowledge of the period of the segmentation clock and the total number of somites formed, we can estimate the average cell-generation time and the total number of PSM cell generations required to generate the full set of somites (Supplementary Box 1). This calculation provides an average cell generation time in the PSM that is much longer in corn snake (~24.4 h) than in mouse (~8 h), chicken (~6.3 h) or zebrafish (~5.5 h). Direct cell-cycle measurements, using 5-bromodeoxyuridine (BrdU) incorporation followed by flow cytometry, gave a cycle time of ~34 h in corn snake embryonic tail and ~30 h in lizard, compared to ~9 h in chicken (as measured using tritiated thymidine[25]; Supplementary Table 4, Fig. 4f and Supplementary Fig. 5), confirming that the cell generation time is almost fourfold slower in snake and lizard than in chicken. Remarkably, the calculated number of cell generations required to generate the 315 somites in the snake (~21 generations) is only slightly greater than for the 65 somites in the mouse (~17 generations) or 55 somites in the chicken (~13 generations), although much larger than for the 31 somites in the zebrafish (~2.8 generations). Therefore, the exceptionally large number of somites in the snake, compared with that in other amniotes, is not primarily the result of a large number of generations of PSM growth, but reflects a clock rate that is rapid in relation to the cell-cycle rate in the elongating axis.

Finally, we investigated the basis for the unusually large number of *LFNG* stripes observed in snake embryos. The number of stripes of expression reflects the number of clock cycles by which the cells at the anterior end of the PSM lag behind those in the posterior PSM. By measuring the stripe spacing, one can deduce how the clock rate changes with position in the PSM[26]. Using measurements of *LFNG* stripe spacing in corn snake embryos, we obtained a graph depicting the slowing down of gene oscillations in the PSM. The graphs for snake and zebrafish are almost identical (Fig. 4g), suggesting that the mechanism controlling the slowing down of cyclic gene oscillations is similar in the two species. The same manner of slowing down of gene oscillations in snake and zebrafish entails very different numbers of PSM stripes simply because of the different ratios of oscillator rate to growth rate (Supplementary Box 2). The faster the oscillator runs relative to PSM growth rate, the more stripes of cyclic gene expression are observed in the PSM.

Thus, our data show that the basic clock-and-wavefront mechanism operates according to similar principles in snake, chicken, mouse and zebrafish. In all four species, somitogenesis ends with a progressive shrinking of the PSM. This shrinking presumably reflects a gradual extinction of the signals that maintain the PSM character of cells at the tail end of the embryo[27]. In chicken and mouse embryos, termination of somitogenesis is an active process associated with extensive cell death in the tail bud[28]. Apoptosis of tail bud cells leading to axis truncation can be induced by retinoic acid treatment[29];

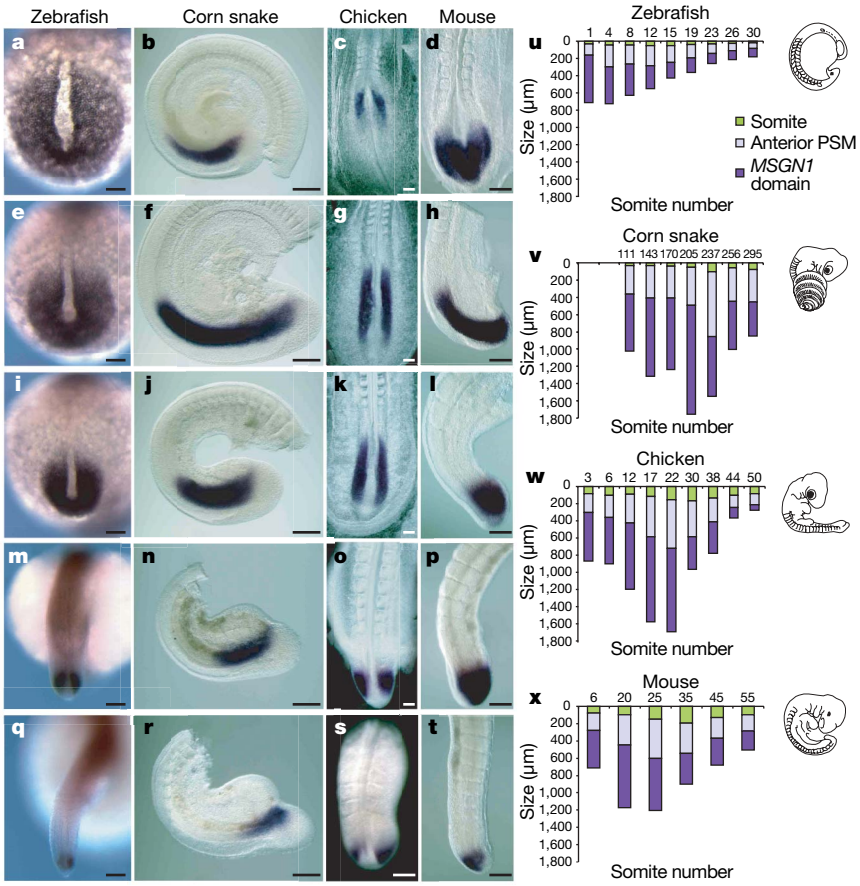

Figure 3 | Dynamics of the PSM size in zebrafish, corn snake, chicken and mouse. a–t, Developmental series of four vertebrate species hybridized with *MSGN1* in whole mount. Zebrafish embryos are shown at 1 (**a**), 8 (**e**), 12 (**i**), 19 (**m**) and 30 (**q**) somites; corn snake embryos at 165 (**b**), 202 (**f**), 251 (**j**), 291 (**n**) and 310 (**r**) somites; Chicken embryos at 6 (**c**), 17 (**g**), 22 (**k**), 30 (**o**) and 44 (**s**) somites; and mouse embryos at 6 (**d**), 20 (**h**), 35 (**l**), 45 (**p**) and 55 (**t**) somites. Dorsal views (**a**, **e**, **i**, **m**, **q**, **c**, **g**, **k**, **o**, **s**, **d**) and lateral views (**b**, **f**, **j**, **n**, **r**, **h**, **l**, **p**, **t**). Anterior to the top. Scale bars correspond to 100 μm (zebrafish) and 200 μm (corn snake, chicken and mouse). **u–x**, Graphs showing the time evolution (in somite numbers) of the PSM (blue), of the somite s_1 (green) and the *MSGN1* domain (dark blue) sizes in chicken, corn snake, mouse and zebrafish embryos.

thus, it is possible that the proximity of the anterior retinoic acid domain to the tail bud caused by PSM shrinking triggers the death of paraxial mesoderm precursors. Therefore, PSM shrinking could explain the arrest of axis elongation and termination of somitogenesis. In zebrafish, the switch to PSM shrinkage occurs very early in comparison with that in amniotes, and this correlates with a small somite number. In amniotes, the switch to PSM shrinkage occurs at the transition between the trunk and the tail region, suggesting that it might be under the control of regional regulators such as *HOX* genes.

Our modelling suggests that the number of PSM generations for which somitogenesis continues changes relatively little among amniotes. In contrast, over the course of evolution there have been large changes in the ratio of the segmentation clock rate to the developmental growth rate. Variation in this ratio accounts for much of the evolutionary divergence in amniote segment number.

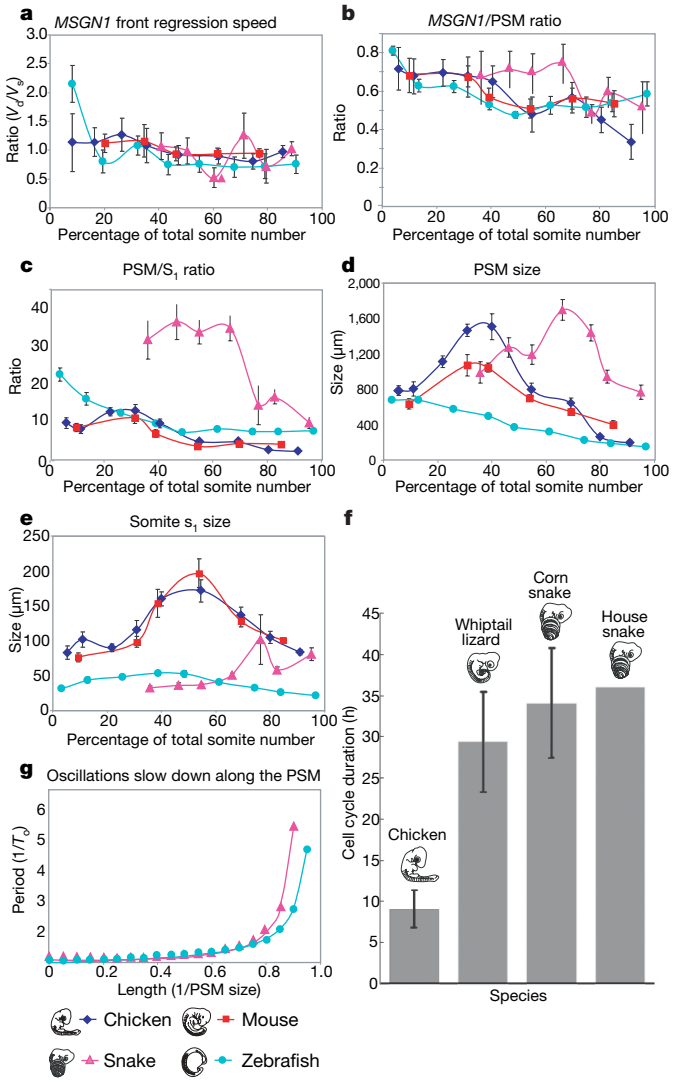

Figure 4 | Comparison of somitogenesis parameters. **a**, Ratio of the speed of the *MSGN1* front regression (in μm per period, V_d) to the speed of somitogenesis (in μm per period, V_s). **b**, Variation of the ratio of the *MSGN1* domain size to the PSM size during somitogenesis. **c**, Variation of the ratio of PSM size to s_1 size during somitogenesis. **d**, Dynamics of the PSM size during somitogenesis. **e**, Dynamics of s_1 size during somitogenesis. **f**, Graph comparing the cell-cycle time in four amniote species. Error bars represent standard deviation. Sample sizes are provided in Supplementary Methods (**a**–**e**) and in Supplementary Table 4 (**f**). **g**, Slowing down of the oscillation period along the PSM (T_o, clock period at the tip of the tail).

METHODS SUMMARY

In total, 192 corn snake eggs, 13 house snake eggs and 34 whiptail lizard eggs were used in this study. Corn snake genes were cloned by PCR using standard protocols (Supplementary Table 1). Orthology was established by calculating the percentage of similarity with orthologous genes in other vertebrate species using Vector NTI (Supplementary Table 2). Whole-mount *in situ* hybridization was performed as described[30] with a hybridization temperature of 58 °C (Supplementary Table 3). For measurements, embryos were hybridized with a *MSGN1* probe in whole mount and were photographed. The size in micrometres of the PSM, the somite s_1 and the *MSGN1* domain were measured using Zeiss LSM image browser software. Embryos were pooled in groups of five on the basis of their somite number. Measurements corresponding to each pool were averaged, and the standard deviation calculated. For the calculation of the slowing down of the period along the PSM in corn snake, interstripe distance was measured using the Zeiss LSM software in two-day post-oviposition embryos (n=23) stained with *LFNG*, and calculations were performed as described[26]. Cell cycle length was measured using BrdU incorporation followed by flow cytometry analysis. Alizarin staining was performed according to standard procedures.

Received 4 October 2007; accepted 21 April 2008.
Published online 18 June 2008.

1. Cooke, J. & Zeeman, E. C. A clock and wavefront model for control of the number of repeated structures during animal morphogenesis. *J. Theor. Biol.* **58,** 455–476 (1976).
2. Palmeirim, I., Henrique, D., Ish-Horowicz, D. & Pourquié, O. Avian *hairy* gene expression identifies a molecular clock linked to vertebrate segmentation and somitogenesis. *Cell* **91,** 639–648 (1997).
3. Dequeant, M. L. & Pourquié, O. Segmental patterning of the vertebrate embryonic axis. *Nature Rev. Genet.* **9,** 370–382 (2008).
4. Dequeant, M. L. *et al.* A complex oscillating network of signaling genes underlies the mouse segmentation clock. *Science* **314,** 1595–1598 (2006).
5. Dubrulle, J., McGrew, M. J. & Pourquie, O. FGF signaling controls somite boundary position and regulates segmentation clock control of spatiotemporal *Hox* gene activation. *Cell* **106,** 219–232 (2001).
6. Sawada, A. *et al.* Fgf/MAPK signalling is a crucial positional cue in somite boundary formation. *Development* **128,** 4873–4880 (2001).
7. Aulehla, A. *et al. Wnt3a* plays a major role in the segmentation clock controlling somitogenesis. *Dev. Cell* **4,** 395–406 (2003).
8. Aulehla, A. *et al.* A β-catenin gradient links the clock and wavefront systems in mouse embryo segmentation. *Nature Cell Biol.* **10,** 186–193 (2008).
9. Richardson, M. K., Allen, S. P., Wright, G. M., Raynaud, A. & Hanken, J. Somite number and vertebrate evolution. *Development* **125,** 151–160 (1998).
10. Delfini, M. C., Dubrulle, J., Malapert, P., Chal, J. & Pourquie, O. Control of the segmentation process by graded MAPK/ERK activation in the chick embryo. *Proc. Natl Acad. Sci. USA* **102,** 11343–11348 (2005).
11. Wittler, L. *et al.* Expression of *Msgn1* in the presomitic mesoderm is controlled by synergism of WNT signalling and *Tbx6*. *EMBO Rep.* **8,** 784–789 (2007).
12. Nakajima, Y., Morimoto, M., Takahashi, Y., Koseki, H. & Saga, Y. Identification of Epha4 enhancer required for segmental expression and the regulation by Mesp2. *Development* **133,** 2517–2525 (2006).
13. Niederreither, K., Subbarayan, V., Dolle, P. & Chambon, P. Embryonic retinoic acid synthesis is essential for early mouse post-implantation development. *Nature Genet.* **21,** 444–448 (1999).
14. Diez del Corral, R. *et al.* Opposing FGF and retinoid pathways control ventral neural pattern, neuronal differentiation, and segmentation during body axis extension. *Neuron* **40,** 65–79 (2003).
15. Burgess, R., Cserjesi, P., Ligon, K. L. & Olson, E. N. Paraxis: a basic helix–loop–helix protein expressed in paraxial mesoderm and developing somites. *Dev. Biol.* **168,** 296–306 (1995).
16. Mansouri, A. *et al.* Paired-related murine homeobox gene expressed in the developing sclerotome, kidney, and nervous system. *Dev. Dyn.* **210,** 53–65 (1997).
17. Yoon, J. K. & Wold, B. The bHLH regulator pMesogenin1 is required for maturation and segmentation of paraxial mesoderm. *Genes Dev.* **14,** 3204–3214 (2000).
18. Sassoon, D. *et al.* Expression of two myogenic regulatory factors myogenin and MyoD1 during mouse embryogenesis. *Nature* **341,** 303–307 (1989).
19. Pownall, M. E. & Emerson, C. P. J. Sequential activation of three myogenic regulatory genes during somite morphogenesis in quail embryos. *Dev. Biol.* **151,** 67–79 (1992).
20. Yoon, J. K., Moon, R. T. & Wold, B. The bHLH class protein pMesogenin1 can specify paraxial mesoderm phenotypes. *Dev. Biol.* **222,** 376–391 (2000).
21. McGrew, M. J., Dale, J. K., Fraboulet, S. & Pourquie, O. The *lunatic Fringe* gene is a target of the molecular clock linked to somite segmentation in avian embryos. *Curr. Biol.* **8,** 979–982 (1998).
22. Forsberg, H., Crozet, F. & Brown, N. A. Waves of mouse *Lunatic fringe* expression, in four-hour cycles at two-hour intervals, precede somite boundary formation. *Curr. Biol.* **8,** 1027–1030 (1998).
23. Zug, G. R., Vitt, L. J. & Caldwell, J. P. *Herpetology: an Introductory Biology of Amphibians and Reptiles* 2nd edn (Academic, San Diego, 2001).
24. Tam, P. P. The control of somitogenesis in mouse embryos. *J. Embryol. Exp. Morphol.* **65** (Suppl), 103–128 (1981).

25. Primmett, D. R., Norris, W. E., Carlson, G. J., Keynes, R. J. & Stern, C. D. Periodic segmental anomalies induced by heat shock in the chicken embryo are associated with the cell cycle. *Development* **105,** 119–130 (1989).
26. Giudicelli, F., Ozbudak, E. M., Wright, G. J. & Lewis, J. Setting the tempo in development: an investigation of the zebrafish somite clock mechanism. *PLoS Biol.* **5,** e150 (2007).
27. Cambray, N. & Wilson, V. Two distinct sources for a population of maturing axial progenitors. *Development* **134,** 2829–2840 (2007).
28. Sanders, E. J., Khare, M. K., Ooi, V. C. & Bellairs, R. An experimental and morphological analysis of the tail bud mesenchyme of the chicken embryo. *Anat. Embryol. (Berl.)* **174,** 179–185 (1986).
29. Shum, A. S. *et al.* Retinoic acid induces down-regulation of *Wnt-3a*, apoptosis and diversion of tail bud cells to a neural fate in the mouse embryo. *Mech. Dev.* **84,** 17–30 (1999).
30. Henrique, D. *et al.* Expression of a *Delta* homologue in prospective neurons in the chicken. *Nature* **375,** 787–790 (1995).

Supplementary Information is linked to the online version of the paper at www.nature.com/nature.

Acknowledgements The authors thank M. Gibson, B. Rubinstein, P. Francois and members of the Pourquié laboratory for critical reading and discussions, M. Wahl for the mouse *LFNG* pictures, members of the Reptile and Aquatics Department, J. Chatfield for editorial assistance, and S. Esteban for artwork. Research was supported by Stowers Institute for Medical Research, and in part by a Defense Advanced Research Projects Agency (DARPA) grant (O.P.). J.L. is supported by Cancer Research UK. Zebrafish were obtained from the Zebrafish International Resource Center (ZIRC) at the University of Oregon, which is supported by a grant from the NIH-NCRR. O.P. is a Howard Hughes Medical Institute Investigator.

Author Contributions C.G. and O.P. designed the experiments, C.G. cloned the snake genes and performed the mouse, chicken and snake *in situ* hybridizations, E.M.O. performed the fish *in situs*, C.G. and E.M.O. performed the measurements and analysed the data with O.P. D.B. established the corn snake and zebrafish colony and produced the embryos. C.G. and J.W. performed the cell cycle analysis. J.L. performed the mathematical modelling. C.G., E.M.O., J.L. and O.P. wrote the manuscript. All authors discussed the results and commented on the manuscript.

Author Information Sequences of genes described in this paper have been deposited into GenBank under accession numbers EU196456, EU196465, EU232010, EU196457, EU196458, EU196459, EU196460, EU196466, EU196461, EU196464, EU196462 and EU196463. Reprints and permissions information is available at www.nature.com/reprints. Correspondence and requests for materials should be addressed to O.P. (olp@stowers-institute.org).